

1 Tempo-spatial variation of the late Mesozoic volcanism in Southeast  
2 China  
3  
4

5 **Xianghui Li<sup>1,2\*</sup> Yongxiang Li<sup>1</sup> Jingyu Wang<sup>1</sup> Chaokai Zhang<sup>1</sup> Yin Wang<sup>3</sup> Ling Liu<sup>3</sup>**

6 <sup>1</sup>*State Key Laboratory for Mineral Deposits Research, School of Earth Sciences and Engineering,*  
7 *Nanjing University, Nanjing 210023 China. Email: [leeschhui@126.com](mailto:leeschhui@126.com)*

8 <sup>2</sup>*State Key Laboratory of Oil and Gas Reservoir Geology and Exploitation, Chengdu University of*  
9 *Technology, Chengdu 610059, China*

10 <sup>3</sup>*East China Mineral Exploration and Development Bureau, Nanjing 210007, China*  
11

## ABSTRACT

The magmatism (including volcanism) in East Asia (/ China) could provide key clues and age constraints for the subduction and dynamical process of the Paleo-Pacific plate. Although lots of absolute isotope ages of extrusive rocks have been published in the 1980s-2000s, large uncertainties and big errors prevent the magmatism in SE China from being well understood. In this study, we investigate the zircon geochronology of extrusive rocks and tempo-spatial variations of the late Mesozoic volcanism in Southeast (SE) China. We reported zircon U-Pb ages of new 48 extrusive rock samples in the Shi-Hang tectonic zone. Together with the published data in recent decade, ages of 291 rock samples from ~40 lithostratigraphic units were compiled, potentially documenting a relatively complete history and spatial distribution of the late Mesozoic volcanism in SE China. The results show that the extrusive rocks spanned ~95 Myr (177-82 Ma), but dominantly ~70 Myr (160-90 Ma), within which the volcanism in the early Early Cretaceous (145-125 Ma) was the most intensive and widespread eruption. We propose that these ages represent the intervals of the Yanshanian volcanism in SE China. Spatially, the age geographic pattern of extrusive rocks shows that both the oldest and youngest age clusters occur in coastal magmatic arc (eastern Zhejiang and Fujian), and the most intensive and widespread age group (145-125 Ma) occurs in back arc / rifting basin (eastern Jiangxi, middle Zhejiang, and northern Guangdong), implying that the late Mesozoic volcanism migrated northwesterly and subsequently retreated southeasterly. This volcanic migration pattern may imply that the Paleo-Pacific plate subducted northwestward and the roll-back subduction did not begin until the Aptian (~125 Ma) of the mid-Cretaceous.

**Keywords:** geochronology; tempo-spatial variation; volcanism; late Mesozoic; Southeast China

## 1. Introduction

It is generally believed that an Andean-type active continental margin had been developed during the late Mesozoic in eastern Eurasia along which the Paleo-Pacific plate (PPP) subducted beneath the East Asia (e.g., Taylor and Hayes, 1983; Faure and Natal'in, 1992; Charvet et al., 1994; Zhou and Li, 2000; Chen et al., 2005; Liu et al., 2017; Li SZ et al., 2019). The subduction has exerted profound impacts in Southeast (SE) China (e.g., Taylor and Hayes, 1983; Zhou and Li, 2000; Li CL et al., 2014; Li JH et al., 2014; Jiang YH et al., 2015; Liu et al., 2016; ) and many other parts of East Asia (e.g., Stepashko, 2006; Wu et al., 2007; Choi and Lee, 2011; Zhang et al., 2011; Sun et al., 2013; 2015; Dong et al., 2016; Liu et al., 2017), as indicated by the pervasive crustal deformation associated with the Yanshanian orogeny (e.g., Lapierre et al., 1997; Li, 2000; Zhou and Li, 2000) and the widespread magmatism (e.g., Zhou et al., 2006; Sun et al., 2007). Obviously, the study of the magmatism would help to constrain the process of the PPP subduction.

The late Mesozoic volcanism in SE China, as a response to the PPP subduction, has long attracted attention, and lots of dating work has been carried out. However, different time intervals and various episodes / cycles / periods of the volcanism have been proposed (e.g., Li et al., 1989; Feng et al., 1993; Zhang, 1997; Guo et al., 2012; Li CL et al., 2014; Liu et al., 2012, 2014, 2016; Jiang SH et al., 2015; Ji et al., 2018; Zhang et al., 2018; Yang et al., 2018; Zhang et al., 2019). The issue can be attributed to: 1) the published ages were generally based on separate and often limited datasets that were commonly from only several to a dozen of samples from a local region such as a mining field, or a province, or at most from a relatively wide area of two neighboring provinces; 2) age data were obtained using different methods, by which, the Rb-Sr, K-Ar, and Ar-Ar dating of bulk-dominated samples yielded ages with large uncertainties and big errors in the 1980s-1990s; 3) refined zircon U-Pb ages of the volcanism have not been analyzed for the whole SE China.

It is essential to obtain spatially more comprehensive datasets from different parts of SE China and also temporally more expanded datasets from sedimentary basin archives that can document the

relatively complete volcanic history to achieve a holistic understanding of the late Mesozoic volcanism and geodynamics in SE China.

In this study, we investigate the geochronology of extrusive rocks in the middle and northern Shi-Hang tectonic belt (SHTB, e.g., Gilder et al., 1996; Jiang et al., 2011; Yang et al., 2012). The SHTB contains thick sedimentary strata, which are interbedded with extrusive rocks, and thus has the advantage of providing a more complete stratigraphic archive that preserves more complete and recognizable volcanic events. We also compile the published zircon U-Pb isotope geochronological data of extrusive rocks from the entire SE China. Obviously, ages of the extrusive rocks can constrain the geochronology of the initiation, evolution, and termination of the late Mesozoic volcanism in SE China. Specifically, we analyze the temporal evolution and the geographical distribution of the late Mesozoic volcanism, which can indirectly help date and better understand the slab subduction between the eastern Asian continent and the western PPP in East Asia (e.g., Gilder et al., 1991, 1996).

## **2. Geological setting**

The South China Block comprises the Yangtze Block and Cathaysia Block. The Yangtze Block has an Archean to Proterozoic basement, whereas the Cathaysia Block has a Proterozoic basement. Yangtze and Cathaysia blocks amalgamated during the early Neoproterozoic Orogeny (e.g., Zhao and Cawood, 1999; Wang et al., 2006; Zheng and Zhang, 2007; Li et al., 2009), forming the Jiangnan orogen. A cover sequence of marine strata from the late Neoproterozoic to the Paleozoic was accumulated on the united South China Block that subsequently underwent the Caledonian orogeny (or the Guangxi movement) in the early Paleozoic (e.g., Guo et al., 1989; Qiu et al., 2000; Charvet et al., 2010) and the Indosinian orogeny in the early Mesozoic (e.g., Carter et al., 2001; Lepvrier et al., 2004).

The major Jiangshan-Shaoxing suture zone separating the Yangtze and Cathaysia blocks (e.g.,

83 Jiang et al., 2011; Yang et al., 2012) had been reactivated during the Indosinian and Yanshanian  
84 movements (e.g., Wang et al., 2013). During the Yanshanian, the Andean-type convergent margin  
85 was developed along the SE China following the subduction of the PPP (e.g., Taylor and Hayes,  
86 1983; Faure and Natal'in, 1992; Charvet et al., 1994; Zhou and Li, 2000; Chen et al., 2005; Liu et al.,  
87 2017; Li SZ et al., 2019). A series of NE-striking back-arc basins associated with widespread and  
88 large-scale magmatism were produced (e.g., Zhou and Li, 2000; Li and Li, 2007; Liu et al., 2014,  
89 2016; Xie et al., 2017; Yang et al., 2017). Since the deposition in these basins was concomitant with  
90 volcanism, it is fairly common that the sedimentary successions are interbedded with volcanic rocks.  
91 On the basis of the abundance of volcanic rocks in the strata, these basins can be grouped into three  
92 types (Fig. 1): volcanic (-dominated), volcanic-sedimentary, and sedimentary (e.g., Chen et al., 2005;  
93 Shu et al., 2009). These three types of basins are roughly separated by two NE-striking fault zones:  
94 the Jiangshan-Shaoxing fault zone and the Zhenghe-Dapu fault zone (Fig. 1). The volcanic basins  
95 occur SE to the Zhenghe-Dapu fault zone and were formed on the magmatic arc (Lapierre et al.,  
96 1997) along the coastline, i.e., the Coastal zone (CZ). The volcanic-sedimentary basins occur in the  
97 SHTB confined between the two fault zones, and volcanic rocks are typically interbedded and / or  
98 intercalated with sedimentary strata, which had been constructed in the back arc / rifting basin (e.g.,  
99 Gilder et al., 1991; Jiang et al., 2009; 2011). Nevertheless, the late Mesozoic volcanic rocks are  
100 almost absent east to the Yujiang-Yudu fault zone in sedimentary basins and western SHTB basins  
101 (Fig. 1).

102 The large-scale magmatism is evidenced by the occurrence of granitic plutons in both the SHTB  
103 and the CZ stretching over 1000 km along the coastal SE China. These granitic plutons intruded into  
104 the Precambrian basement and the overlying Paleozoic strata during the Middle Jurassic-Early  
105 Cretaceous (e.g., Jiang et al., 2011; Yang et al., 2012). The intrusions mainly occur as A-type and /  
106 or I-type granitic rocks, and together with huge volcanic rocks, strongly support the model of the  
107 western subduction of the PPP (e.g., Zhao et al., 2016; Jiang et al., 2011; Yang et al., 2012; Xie et al.,

108 2017; Yang et al., 2017).

### 109 **3. Material and methods**

110 A total of 48 extrusive rock samples were collected from about 20 lithostratigraphic formations  
111 (supplementary data Table RD1) in 11 basins / regions within the main SHTB to obtain new zircon  
112 U-Pb isotope ages (L1-L10 in Fig. 1; supplementary data Figs. RD1-RD3 and Table RD1). The  
113 extrusive rock specimens are volcanic and pyroclastic rocks that are interbedded and intercalated  
114 with the sedimentary strata, in which sampling horizons and associated lithologies are marked in the  
115 supplementary data figures RD4-RD12. These samples were collected from volcanic layers in the  
116 main type sections of typical basins in SE China (supplementary data Fig. RD4-RD12). In general,  
117 3-4 rock samples were taken at lower/base, middle and upper/top part when a lithostratigraphic unit  
118 has multiple volcanic horizons or a volcanic layer is over 100-200 m thick (see supplementary data  
119 Table RD1). The locations of these samples were determined with a GPS device and are marked on  
120 the geological maps (supplementary data Figs. RD1-RD3 and Table RD1).

121 Zircon grains were separated using the conventional heavy liquid and magnetic techniques.  
122 Single zircon grains were handpicked and mounted on adhesive tapes, embedded in epoxy resin, and  
123 then polished to about half to one-third of their thickness and photographed in both reflected and  
124 transmitted light. Cathodoluminescence (CL) images were taken at the State Key Laboratory for  
125 Mineral Deposits Research, School of Earth Sciences and Engineering, Nanjing University, to  
126 examine the internal structures of single zircon grains before U-Pb isotope analysis.

127 LA-ICP-MS, U-Th-Pb analyses of single zircon grains were performed on a Nd of YAG 213  
128 laser ablation system (Agilent 7500a, New Wave Research, U.S.A.) coupled with VG PQ Excell  
129 ICP-MS, which is housed in the State Key Laboratory for Mineral Deposits Research, Nanjing  
130 University. General ablation time is ca. 60 s and the ablation pit diameter is at 25-35  $\mu\text{m}$ . The  
131 ablation repetition rate is 5 Hz with the incident pulse energy of about 10~20 J/cm<sup>2</sup>. Calibrations of

mass fractionation were made using the index sample GEMOC/GJ (608 Ma). In each experiment, a total of 11 to 21 zircon grains were measured, among which 8 to 18 grains yield concordant age data. Prior to each experiment, the standard GJ-1 and Mud Tank samples were measured. Other measurements follow the methods described by Jackson et al. (2004). Analyses of Mud Tank sample yielded a weighted  $^{206}\text{Pb}/^{238}\text{U}$  age of  $726\pm 10$  Ma~ $737\pm 5$  Ma ( $2\sigma$ ), which is in good agreement with the recommended value (TIMS age =  $732\pm 5$  Ma, Black and Gulson, 1978).

Data reduction, isotope ratio, age calculation, and Pb correction were conducted with the GLITTER software using Zircon 91500 as an external standard. Data processing and plotting were executed with the Isoplot 3.23 programs (Ludwig, 2001). The uncertainties of age results are quoted at  $1\sigma$  confidence level, whereas errors for weighted mean ages are quoted at  $2\sigma$ .

It is worth noting that those aged samples of mafic dykes, basalts and gabbros were not herein compiled for the analysis of volcanic temporal-spatial variation in SE China. This is because: 1) among the magmatic rocks, gabbros and basalts are rare, and diorites and andesites are even less common in South China (Zhou and Li, 2000), leading to a weak significance in statistic of the volcanic samples; 2) those published ages of the dykes, basalts and gabbros were mainly measured using different (Ar-Ar, K-Ar, Rb-Sr) isotopic methods (e.g., Li, et al., 1989; Chen et al., 2008b; Wang et al., 2008; Meng et al., 2012), likely causing chaos of real ages; 3) it is difficult to obtain a good isotopic age for mafic rocks, and particularly, the bulk (basalt) samples ages by K-Ar, Ar-Ar, and Rb-Sr are ~ 10-20 Ma younger than those by zircon U-Pb isotopes (Li et al., 2019); and 4) some basalts predominantly are of the Indosinian orogeny age, instead of the Yanshanian orogeny.

## **4. Results**

### **4.1 Uncertainty of zircon U-Pb ages**

It is necessary to first evaluate the uncertainty of the new age results and other cited age data. The uncertainty depends on three aspects, i.e. origin of zircon, precision, and accuracy (Schoene et al., 2013).

157 For the origin, all zircons used in this work were microscopically evaluated with CL to ensure  
158 that laser ablation positions of zircons are away from the nucleus, cracks, and inclusions. CL images  
159 manifest the growth rings. In the concordant 636 zircons of this work, 20 grains (3.1%) are 0.1-1.0 in  
160 Th/U ratio, 615 (96.7%) are 1.0-10.0 (Table 1). Th/U ratios of 3539 zircons can be available in the  
161 age data from published references. Together with published data and this work, 1766 zircon grains  
162 (42.3%) are 0.1-1.0 in Th/U ratio, 2394 grains (57.3%) are 1.0-10.0, 14 grains (0.3%) are > 10.0, and  
163 only one is less than 0.1 (Table 1). CL images and Th/U ratios of this work combined the collected  
164 data demonstrate that predominant (>99.9%), if not all, zircons are magmatic origin.

165 Precision and accuracy uncertainties produced during LA-ICP-MS zircon U-Pb dating have been  
166 more and more concerned (e.g., Klötzli et al., 2009; Solari et al., 2010; Li et al., 2015) and come  
167 from multiple sources, including the isotopic ratio measurements, the fractionation factor calculation  
168 using an external standard, the common lead correction, the external standards, and the data  
169 reduction (Li et al., 2015). According to the suggested ~4% ( $2\sigma$ ) of precision and accuracy (Li et al.,  
170 2015), we used the ~2% and ~2-4% ( $1\sigma$ ) to evaluate uncertainties of extrusive rock ages.

171 A total of 48 rock samples were respectively weighed in mean from 636 concordant zircon U-Pb  
172 ages in this work (supplementary data Table RD1 and RD2). In the samples, 46 (95.8%) have a <3  
173 million years (Myr) error in  $1\sigma$ , in which 36 (75%) samples have <2 Myr error in  $1\sigma$ ; 41 samples  
174 (85.4%) have <2.0% (error / age) deviation, and 7 (14.6%) have 2-4% deviation (Table 1). Similar  
175 percentages of sample error and age deviation are comparative with those single zircons analyzed in  
176 this work (Table 1).

177 For zircons from the published data, the literature often provides CL images of zircons showing  
178 quite similar nature in source and error. For the zircon U-Pb ages from the previous studies, we  
179 carefully examine the experiments described in the literature, re-analyze the concordant ages, and  
180 eliminate those that are not concordant and / or greater than ~5% in age deviation (error / age) as  
181 well as ages with distinct inheritance, which were not discarded by the original authors. This



182 scrutinizing procedure allows us to identify reliable U-Pb age data from 188 volcanic rock samples  
183 from the SHTB and from 103 volcanic rock samples from the CZ (supplementary data Table RD2  
184 and RD3). Then, results show that in the combined 291 samples, 246 samples (85.5% = 246/291) are  
185 <2 Myr in  $1\sigma$  error of age and 39 (13.4 %) are 2-4 Myr; and 264 samples (90.7%) are <2.0% age  
186 deviation and 25 (8.6%) are 2-4 Myr deviation in age (Table 1). Closely, total concordant single  
187 zircons 4639 are similar in percentages of  $1\sigma$  error and age deviation with the weighed-mean age  
188 samples (Table 1).

189 The above relatively low errors in  $1\sigma$  and deviation of age indicate that samples of both this and  
190 previous work have highly proportional age results (> ~95%) with fine precision.

191 Systematic biases often dominate uncertainty in comparisons between dating methods and  
192 between laboratories (Schoene et al., 2013). For measurements of our zircon samples, the internal  
193 systematic  $2\sigma$  error is less than 3%, which has been verified by reproductive measurements of Mud  
194 Tank sample (see Section 3). These systematic biases were mostly met for those zircons from the  
195 references. Therefore, small internal systematic  $2\sigma$  errors allow our zircon date results to be a  
196 moderate accuracy in geochronological application.

197 The internal systematic conditions are same for weighted mean dates of individual samples from  
198 both this and previous work (ref. and comp. to supplementary data Table RD1-RD3). Compiled  
199 zircons are predominantly single dates generally within less than 2 Myr in  $1\sigma$  errors (<3% biases) for  
200 the Late Jurassic – Early Cretaceous volcanic rocks. The dates are to great degree consistent with the  
201 biostratigraphy of pollens-spores, plants, ostracods, and conchostracans in the volcanic-sedimentary  
202 basins, SHTB (e.g., Chen and Shen, 1982; Sha, 1990; Jiang et al., 1993; Chen, 2000).

203 In summary, the zircon origin and the age precision and accuracy indicate the sample  
204 weighed-mean ages have relatively low uncertainty and they are eligible for investigating the  
205 eruption geochronology of extrusive rocks in SE China.

## 4.2 U-Pb age spectra of extrusive rocks

Spot analyzing results of this work show that 48 samples have a wide range of (concordant  $^{206}\text{Pb}/^{238}\text{U}$ ) weighed-mean ages from 162 Ma to 92 Ma (green histogram, Fig. 2a), from which two peaks of weighted mean ages are inconspicuously regressed as  $133.3 \pm 1.5$  Ma and  $97.2 \pm 1.1$  Ma, respectively (Fig. 2a). In addition, 636 concordant single zircons from the samples show similar wide age range (166 Ma to 92 Ma) with three age peaks (Fig. 2a.  $135.87 \pm 0.42$  Ma,  $124.71 \pm 0.35$  Ma, and  $98.91 \pm 0.57$  Ma).

Combining our new results with the published age data from the main SHTB (e.g., Wu et al., 2011a, b; Wu and Wu, 2013; Liu et al., 2012, 2014, 2016; Li CL et al., 2014; Li JH et al., 2014; Ma et al., 2016; Wang et al., 2016; Shu et al., 2017. Locations M1-M22, Table RD1 and Fig. 1) yields a similar age pattern (Fig. 2b). A total of 188 rock samples show that the weighed-mean age range from 177 Ma to 92 Ma with distinct age peak  $136.11 \pm 0.38$  Ma and inconspicuous age peak  $100.0 \pm 1.0$  Ma (Fig. 2b). Also, a total of 2593 single zircons from the SHTB show the concordant  $^{206}\text{Pb}/^{238}\text{U}$  ages ranging from 180 Ma to 92 Ma with strong age peak  $132.07 \pm 0.17$  Ma and weak peak  $101.26 \pm 0.23$  Ma (Fig. 2b).

The published data of 103 rock samples from the CZ (for Locations N1-N21, see Fig. 1 and supplementary data Table RD1 and RD3. Chen et al., 2008; Li et al., 2009; Guo et al., 2012; Li CL et al., 2014; Liu et al., 2012, 2016; Zhang et al., 2018) show a wide weighed-mean ages ranging from 174 Ma to 82 Ma and three remarkable age peaks of  $143.15 \pm 0.82$  Ma,  $130.96 \pm 0.87$  Ma, and  $98.13 \pm 0.55$  Ma (Fig. 2c), similar to those from the SHTB (comp. Fig. 2b and 2c). The 2046 single zircons from the 103 samples also display the same range of concordant  $^{206}\text{Pb}/^{238}\text{U}$  ages (Fig. 2c; supplementary data Table RD3) with two prominent age peaks ( $131.04 \pm 0.32$  Ma and  $99.08 \pm 0.32$  Ma. Fig. 2c).

Further combined and optimized age data of 291 extrusive rock samples of over 40 lithostratigraphic units in both SHTB and CZ illustrate that sample weighed-mean ages mainly vary

231 between 177 Ma and 82 Ma (Fig. 3). Of the ages, two peaks are at  $132.86 \pm 0.46$  Ma (75 samples,  
232 138-130 Ma, MSWD = 2.3) and  $98.19 \pm 0.47$  Ma (25 samples, 100-96 Ma, MSWD = 1.14),  
233 respectively. The compilation of age data from all the 4639 concordant single zircons shows that the  
234  $^{206}\text{Pb}/^{238}\text{U}$  ages range between ~180 Ma and ~76 Ma with two age peaks at  $132.90 \pm 0.14$  Ma and  
235  $99.86 \pm 0.19$  Ma (Fig. 3).

## 236 **5. Discussion**

### 237 **5.1 Temporal evolution of volcanism**

238 The late Mesozoic extrusive rocks are widespread in SE China and their dating has been  
239 conducted extensively. In early times, they have been roughly dated as the (Late) Jurassic and (to the  
240 Late) Cretaceous by the confinement of interbedded / intercalated terrestrial fossil-bearing  
241 sedimentary strata, and the ages are quite crude. Later on, Rb-Sr, K-Ar, and Ar-Ar dating of  
242 bulk-dominated samples yielded ages of ~150-65 Ma with large age uncertainties in the 1980s-1990s  
243 (e.g., Hu et al., 1982; Li et al., 1989; Feng et al., 1993; Zhang, 1997), much younger than the earlier  
244 rough estimates, and ~10-20 Myr younger than the zircon U-Pb isotope ages on average (Li et al.,  
245 2019).

246 In the recent decade, though zircon U-Pb age data of the igneous rocks have been reported, rock  
247 samples in individual references were taken from separate locations resulting in different age  
248 interpretations of volcanic eruption in SE China, and a relative concurrent viewpoint has not been  
249 reached. Multiple volcanic age durations are available at different locations or regions, such as  
250 145-129 Ma, 143-98 Ma, and 140-118 Ma in eastern and northwestern Zhejiang (Liu et al., 2014),  
251 140-88 Ma and 136-129 Ma in southeastern (Liu et al., 2012) and central Zhejiang (Li JH et al.,  
252 2014), 168-95 Ma in northeastern Guangdong and southeastern Fujian (Guo et al., 2012), 162-130  
253 Ma from two locations in Fujian (Li et al., 2009), 160-99 Ma from northern Fujian (Liu et al., 2016),  
254 and 112-99 Ma from Zijingshan Mineral Field of Fujian (Jiang et al., 2013, 2015). Obviously, these  
255 ages are incomplete and intermittent, and cannot individually reveal the age of volcanism in the

256 entire SE China.

257 To investigate the geochronology of extrusive rocks, we conducted zircon U-Pb age analysis in  
258 the SHTB and combined the published data from both SHTB and CZ. Then relatively high precise  
259 and representative dating results are obtained in entire SE China: the combined and optimized ages  
260 from 291 rock samples (4639 concordant zircons) range from ~177 Ma to ~82 Ma (mainly 160-90  
261 Ma).

262 As we know, the U-Pb isotope ages of zircons represent the cease time of the crystalline zircon  
263 formation when volcanic eruption, therefore, we propose that the age range above is an eligible  
264 representation for the duration of volcanism in SE China. That means, the volcanism could have  
265 initiated at the late Toarcian (~177 Ma) of the late Early Jurassic and terminated at the early  
266 Campanian (~82 Ma) of the Late Cretaceous, and it has a ~95 Myr duration, which shows little  
267 discrepancy with those of the single zircon ages (Fig. 3). On the other hand, the volcanism occurred  
268 chiefly during the interval of the Late Jurassic-early Late Cretaceous (160-90 Ma = 70 Myr) when  
269 only several samples with ages of pre-160 Ma and post-90 Ma are disregarded (e.g., Chen et al.,  
270 2007; Guo et al., 2012; Liu et al., 2012). When consider the relationship of the magmatism to the  
271 Yanshanian origination, the above age range and duration (~177-82 Ma) probably represent the time  
272 of the Yanshanian orogeny in East and SE Asia.

273 Then the temporal evolution scenario of the volcanism in SE China can be summarized as (Fig.  
274 3): 1) during the latest Early Jurassic (late Toarcian) - Latest Late Jurassic (~177-145 Ma), the  
275 volcanism was sporadic; 2) the early Early Cretaceous (Berriasian-Barremian, ~145-125 Ma)  
276 volcanic eruption was the most intensive; 3) and the volcanism became fading during the main  
277 mid-Cretaceous (Aptian-Turonian, ~125-92 Ma); 4) the volcanism almost ceased since then (~92-82  
278 Ma). The most extensively volcanic eruption episode (145-25 Ma) seems to correspond to the period  
279 of rapid increase in the magmatic flux of both the Mid-ocean ridge and Large Igneous Provinces  
280 (Coffin & Eldholm, 1994) during the late Late Jurassic-early Early Cretaceous (Fig. 4) although the

relationship between them remains unclear.

It is noted that among the compiled single zircon U-Pb ages of extrusive rocks, the oldest one is from the Maonong Formation in the Songyang Basin, southwestern Zhejiang. The weighted mean age is  $177.4 \pm 1.0$  Ma for the sample MN01 (location M14. Liu et al., 2012). In addition, a weighted mean age of  $180 \pm 4$  Ma from the same horizon (Chen et al., 2007) has also been reported despite that the error is relatively large, up to 6-8 Myr.

Similarly, variable youngest ages of volcanic rocks are reported. The weighted mean age of  $82.5 \pm 1.0$  Ma of the sample ZJ23 (location N2. Chen et al., 2008) from the Taozu section of eastern Zhejiang could be the youngest age. One zircon grain from the section is dated at  $74 \pm 0.6$  Ma and five zircon grains yield concordant ages of  $76 \pm 0.6$  Ma from the same sample (Table RD3. Chen et al., 2008), suggesting that it is possible the termination of volcanism was ~5 Myr younger than 82.5 Ma.

Two hiatuses volcanism at 128-122 Ma and 120-110 Ma were recently proposed in eastern Zhejiang (Liu et al., 2012), and volcanic reticence of 130-115 Ma was reported in northeastern Guangdong and southeastern Fujian (Guo et al., 2012. N17, N19, N20 in figure 1). Similar silence / inactiveness of volcanism seems happened in other parts of SE China. However, this volcanic silence is a gloss, and it would not have happened when we see all the late Mesozoic volcanism in SE China.

## **5.2 Spatial pattern of volcanism**

Though it is well-known that the late Mesozoic magmatic rocks are widespread in SE China, the previous volcanic distributions are to some degree out of date as those ages contain large errors with low preciseness and accuracy by bulk isotope dating (e.g., Li et al., 1989; Wang et al., 2000; Zhou and Li, 2000; Chen et al., 2008b) and detailed age distribution patterns by precise age constraints have not been outlined yet. To delineate the spatial variation of the late Mesozoic volcanism in SE China that are refined by the zircon U-Pb geochronology, we sketched three distribution maps of

305 extrusive rocks by the initial, peak, and terminal ages of volcanism (Fig. 5a, 5b, and 5c).

306 Firstly, we identified the initial ages of extrusive rocks. The initial age is defined as the earliest  
307 age of volcanic eruption in a location, a basin, and / or a region marked as capital letters L, M and N  
308 with numbers in figure 1. Three age boundaries ~163 Ma, ~145 Ma, and ~125 Ma are chosen to  
309 divide the initial ages into four intervals: 177-163 Ma, 163-145 Ma, 145-125 Ma, and <125 (-94) Ma,  
310 ordinarily corresponding to the epochs of the Middle and Late Jurassic, the early and late Early  
311 Cretaceous, respectively. We used the boundary age 177 Ma as the earliest boundary within the first  
312 period of the volcanism because it could represent the initiation time of the first Yanshanian orogenic  
313 episode in SE China and the corresponding stratal boundary is marked by an unconformity (e.g., Yu  
314 et al., 2003; Shu et al., 2009). The boundary between the Upper Jurassic and the Lower Cretaceous is  
315 also represented by a widely observed unconformity (e.g., Yu et al., 2003; Shu et al., 2009) and the  
316 intensification of volcanism in SE China (Fig. 3). As there are fewer samples with ages of < 125 Ma  
317 and the age boundary at ~125 Ma marks the rapid waning of volcanism (Fig. 3), we designed the  
318 interval 125-94 Ma of volcanism as the latest initial age recognition.

319 Then, isolines ages are drawn by the boundary age 163 Ma, 145 Ma, and 125 Ma, separately.  
320 Interpolation ages are used to confine the zones when there are no exact ages same as the boundary  
321 age occur in the map. Plotting the initial ages in the geographical map shows four zones of initial  
322 volcanism in SE China (Fig. 5a). Zone 1 (Middle Jurassic, 177-163 Ma) marks areas where initial  
323 volcanic eruption locally occurs in the northernmost corner of Guangdong and neighboring southern  
324 corner of Fujian as well as northeastern corner of Fujian and at one location of southwestern  
325 Zhejiang (M14, Songyang, Liu et al., 2012). Zone 2 (Late Jurassic, 163-145 Ma) delineates areas  
326 where initial volcanic eruption occurs around Zone 1 in southern and northeastern Fujian with a  
327 much larger scope in southern Fujian than Zone 1. Zone 3 (early Early Cretaceous, 145-125 Ma)  
328 defines regions where initial volcanic eruption chiefly and largely extends in SE China, and mostly  
329 bounded in west of the volcanic area, extending along the eastern Jiangxi, northwestern Fujian, and

330 middle Zhejiang (Fig. 5a). Zone 4 (late Early Cretaceous, 125-94 Ma) locally occupies eastern  
331 Zhejiang and limited southeastern Fujian (south of Fuzhou). Same zones can be also recognized in  
332 the map made from the single zircon U-Pb ages (comp. the supplementary data Fig. RD13),  
333 supporting the zonations of the sample weighed-mean ages.

334 Secondly, the peak eruption age of extrusive rocks can be identified, which is defined as the  
335 main age of extensively volcanic eruption in a location, a basin, and / or a region marked with L, M  
336 and N with numbers in figure 1. Here we use 145 Ma, 125 Ma, and 100 Ma as three boundary ages to  
337 differentiate the most extensive volcanism in SE China. This is because the main ages are much  
338 younger than 145 Ma and few samples show ages younger than 100 Ma, for which the main age  
339 isolines are more readily made. Similarly, the corresponding age intervals confined by the boundary  
340 ages pertain to the epochs of the Late Jurassic, the early and late Early Cretaceous, and early Late  
341 Cretaceous, respectively.

342 Isolines of boundary ages are delineated by 145 Ma, 125 Ma, and 100 Ma and completed with  
343 interpolation ages when no exact ages in the transition zone. Four zones of peak volcanism are then  
344 shown in the geographical map, SE China (Fig. 5b). Zone 1 (Late Jurassic, 163-145 Ma) is the area  
345 where most intensively volcanic eruption occurred in southeastern and northeastern Fujian and  
346 locally at a place in southwestern Zhejiang (Fig. 5b). Zone 2 (early Early Cretaceous, 145-125 Ma)  
347 largely extends along the eastern Jiangxi, middle Zhejiang, northwestern Fujian, and northern  
348 Guangdong (Fig. 5b) and indicates widespread volcanism in SE China. Zone 3 (late Early Cretaceous,  
349 125-100 Ma) occurs as a band in middle Zhejiang, southern Fujian, and northeastern Guangdong.  
350 Zone 4 (early Late Cretaceous, 100-76 Ma) locally distributes along Zone 3.

351 Thirdly, we use the terminal eruption age of extrusive rocks to represent the termination time of  
352 the last volcanism, which is helpful to distinguish the terminal volcanic distribution in SE China. The  
353 age boundaries and intervals are the same as the peak eruption. It is noted that only one age is older  
354 than 145 Ma in northeastern corner of Fujian and lots of samples are younger than 100 Ma.

355 With the confinement of boundary age 145 Ma, 125 Ma, and 100 Ma, age isolines are drawn  
356 separately, and interpolation method was used to confine the zones when there are no exact ages in  
357 the map. Four age zones of the terminal volcanism are recognized in the geographical map by the age  
358 isolines (Fig. 5c). Zone 1 (>145 Ma) occurs in northeastern corner of Fujian due to only one location  
359 of the terminal age. Zone 2 (145-125 Ma) mainly occurs in eastern Jiangxi and banded boundary of  
360 northern Fujian; Zone 3 (125-100 Ma) largely distributes in the boundary region of eastern Jiangxi  
361 and western Fujian and in middle and southwestern Zhejiang. Zone 4 (100-83 Ma) widely appears in  
362 regions of the middle Fujian, eastern Zhejiang, and northern Guangdong. Similar zonations can be  
363 classified in the map sketched by the single zircon U-Pb ages (supplementary data Fig. RD14),  
364 verifying the zones of the sample weighed-mean ages in SE China.

365 Zonations of initial, peak, and terminal volcanism indicate a distinct pattern of volcanic  
366 extrusion in SE China (Figs. 5): the oldest ages in the eastern SE China, the younger intensive age  
367 clusters in the western SE China and the youngest ones in eastern SE China again. Detailed  
368 distributional patterns can be observed: 1) the earliest appearance and earliest disappearance of  
369 extrusive rocks dominantly occur in southeastern and northeastern Fujian, where the magmatic arc  
370 was located (e.g., Lapierre et al., 1997); 2) the most widespread distribution of extrusive rocks is the  
371 most intensive volcanism age as 145-125 Ma in eastern Jiangxi, middle Zhejiang, and northern  
372 Guangdong, in which a back-arc / rifting basin was developed (e.g., Gilder et al., 1991; Jiang et al.,  
373 2009; 2011); 3) the latest appearance and latest disappearance mainly occur in eastern Zhejiang,  
374 eastern Fujian, and northern Guangdong.

375 With the observation of volcanism, two distributional patterns manifest: 1) the migration of the  
376 volcanism was from the northwestward to the southeastward, implying that the PPP could have been  
377 subducted northwestly during the late Mesozoic time; 2) the first appearance (initial volcanism) area  
378 and the first disappearance (terminal volcanism) region are the same region, suggesting that a  
379 roll-back subduction of the PPP happened after ~125 Ma.



380 It is surprising that the zone 1 and / or 2 of volcanism look like thermal-dome patterns (Fig. 5)  
381 by exhumation and exposure that may be related to the regional magmatic intrusion, likely  
382 misleading the migration of volcanism. However, the distribution pattern is not dome-controlled  
383 because: 1) The data are derived from extrusive rocks, instead of intrusive rocks; 2) it is impossible  
384 that a crater is over 200-300 km wide in diameter; 3) lots of agglomerates representing craters were  
385 observed in a variety of strata at locations / basins out of Zone 1. For instance, these agglomerates  
386 are widespread in basins of western Zhejiang (L1~L4; M9~M14), eastern Jiangxi (L5~L7;  
387 M16~M18b), and western Fujian (L8~L10, M19~M22).

## 388 **6. Conclusions**

389 We analyzed weighed mean ages of 48 extrusive rock samples (total of 636 concordant single  
390 zircons) from ~20 lithostratigraphic units at 11 localities in the SHTB. Published ages of 243 rock  
391 samples (total of concordant 4003 zircons) from ~40 lithostratigraphic units in SE China are  
392 compiled and re-examined. Based on a total of refined 291 sample ages (4639 concordant zircon  
393 U-Pb ages) from this study and the published literatures, we propose that the late Mesozoic  
394 volcanism in SE China initiated at ~177 Ma (late Toarcian of the late Early Jurassic) and terminated  
395 at ~82 Ma (early Campanian of the Late Cretaceous), spanning an ~95 Myr interval (mainly ~70 Myr  
396 = 160-90 Ma), during which the 145-125 Ma (the early Early Cretaceous) volcanism is the most  
397 intensive and widespread magmatic eruption. These age range and span may represent the time of the  
398 Yanshanian magmatism in SE China.

399 Isolines of initial, peak, and terminal volcanic ages are drawn to outline the geographic  
400 distribution of extrusive rocks in SE China. The volcanic extrusion age spatial change shows a  
401 distinct pattern of the late Mesozoic volcanism: both the oldest and youngest ages in eastern (coastal)  
402 Zhejiang and Fujian (magmatic arc), and the most intensive and widespread ages in eastern Jiangxi,  
403 middle Zhejiang and northern Guangdong (back arc / rifting basin), hundreds of kilometers away  
404 from the coast line. The geographical distribution pattern of the volcanic eruption ages indicates a

migration process of magmatic extrusion in SE China and implies that a northwestern subduction of the Paleo-Pacific plate happened and a possible roll-back subduction did not begin until the Aptian (~125 Ma) of the mid-Cretaceous.

## Acknowledgments

We thank Ke Cao, Sijing Liang, Yannan Ji, Sihe Wang for participating the field investigation. We are grateful to the reviewers (xxxxxxx) for their helpful comments and constructive suggestions. This research was supported by National Key R & D Plan (Grant 2017YFC06014005), Natural Science Foundation of China (NSFC) projects 41372106 and 41672097, and National Basic Research Program of China (973 Project) 2012CB822003.

## References cited

- Black, L. P., and Gulson, B. L.: The age of the Mud Tank carbonatite, Strangways Range, Northern Territory: BMR, J. Aust. Geol. Geophys., 3, 227-232, 1978.
- Carter, A., Roques, D., and Bristow, C.: Understanding Mesozoic accretion in Southeast Asia: Significance of Triassic thermotectonism (Indosinian orogeny) in Vietnam, Geology, 29, 211-214, 2001.
- Charvet, J., Lapierre, H., and Yu, Y. W.: Geodynamic significance of the Mesozoic volcanism of southeastern China, J. SE Asian Earth Sci., 9, 387-396, 1994.
- Charvet, J., Shu, L. S., Faure, M., Choulet, F., Wang, B., Lu, H. F., and Le Breton, N.: Structural development of the Lower Paleozoic belt of South China: genesis of an intracontinental orogen, J. Asian Earth Sci., 39, 309-330, 2010.
- Chen, C. H., Lee, C. Y., and Shinjo, R.: Was there Jurassic paleo-pacific subduction in South China?: constraints from  $^{40}\text{Ar}$ - $^{39}\text{Ar}$  dating, elemental and Sr-Nd-Pb isotopic geochemistry of the Mesozoic basalts, Lithos, 106, 83-92, 2008b.
- Chen, C. H., Lee, C. Y., Lu, H. Y., and Hseh, P. S.: Generation of Late Cretaceous silicic rocks in SE China: Age, major element and numerical simulation constraints, J. Asian Earth Sci., 31, 479-498, 2008.
- Chen, C. H., Lin, W., Lan, C. Y., and Lee, C. Y.: Geochemical, Sr and Nd isotopic characteristics and tectonic implications for three stages of igneous rock in the late Yanshanian (Cretaceous)

orogeny, SE China, *Geol. Soc. Am., Special Paper*, 389, 237-248, 2005.

Chen, P. J., and Shen, Y. B.: The Late Mesozoic conchostracan fossils in Jiangsu, Zhejiang and Anhui provinces, *Palaeont. Sin. China*, 161(17), 2-27 (in Chinese with English abstract), 1982.

Chen, P. J.: The classification and correlation of non-marine Jurassic and Cretaceous of China: *Comment. J. Stratig.*, 24(2), 114-119 (in Chinese with English abstract), 2000.

Chen, R., Xing, G. F., Yang, Z. L., Zhou, Y. Z., Yu, M. G., and Li, L. M.: Early Jurassic zircon SHRIMP U-Pb age of the dacitic volcanic rocks in the southeastern Zhejiang Province determined firstly and its geological significances, *Geol. Rev.*, 53(1), 31-35 (in Chinese with English abstract), 2007.

Chen, W. F., Chen, P. R., Xu, X. S., and Zhang, M.: Geochemical characteristics of Cretaceous basaltic rocks in South China and constraints on Pacific Plate subduction, *Sci. China (Series D)*, 48(12), 2104-2117, 2005.

Choi, T., and Lee Y. I.: Thermal histories of Cretaceous basins in Korea: Implications for response of the East Asian continental margin to subduction of the Paleo-Pacific Plate, *Island Arc*, 20, 371-385, 2011.

Coffin, M. F., and Eldholm, O.: Large igneous provinces: Crustal structure, dimensions, and external consequences. *Rev. Geophys.*, 32, 1-36, 1994.

Dong, Y., Ge, W. C., Yang, H., Xu, W. L., Zhang, Y. L., Bi, J. H., Liu, X. W.: Geochronology, geochemistry, and Hf isotopes of Jurassic intermediate-acidic intrusions in the Xing'an Block, northeastern China: Petrogenesis and implications for subduction of the Paleo-Pacific oceanic plate. *J. Asian Earth Sci.*, 118, 11-31, 2016.

Faure, M., and Natal'in, B.: The geodynamic evolution of the eastern Eurasian margin in Mesozoic times, *Tectonophysics*, 208, 397-411, doi: 10.1016/0040-1951(92)90437-B, 1992.

Feng, Z. Z.: Mesozoic volcanism and tectonic environments in Fujian, *Reg. Geol. China*, 4(4), 311-316 (in Chinese with English abstract), 1993.

Gilder, S. A., Gill, J., and Coe, R. S.: Isotopic and paleomagnetic constraints on the Mesozoic tectonic evolution of South China. *J. Geophys. Res.*, 101, 16137-16154, 1996.

Gilder, S. A., Keller, G. R., and Luo, M.: Eastern Asia and the western Pacific timing and spatial distribution of rifting in China, *Tectonophysics*, 197, 225-243, 1991.

Guo, F., Fan, W., Li, C., Zhao, L., Li, H., and Yang, J.: Multi-stage crust-mantle interaction in SE China: temporal, thermal and compositional constraints from the Mesozoic felsic volcanic rocks in eastern Guangdong-Fujian provinces, *Lithos*, 150, 62-84, 2012.

Guo, L. Z., Shi, Y. S., Lu, H. F., Ma, R. S., Dong, H. G., and Yang, S. F.: The pre-Devonian tectonic patterns and evolution of South China, *J. SE Asian Earth Sci.*, 3, 87-93, 1989.

468 Hu, H. G., Hu, S. L., Wang, S. S., and Zhu, M. Jurassic and Cretaceous age of volcanic rocks on  
 469 isotope dating, *Act Geol. Sin.*, 56(4), 315-322 (in Chinese with English abstract), 1982.

470 Jackson, S. E., Pearson, N. J., Griffin, W. L., and Belousova, E. A.: The application of laser  
 471 ablation-inductively coupled plasma-mass spectrometry to in situ U/Pb zircon geochronology,  
 472 *Chem. Geol.*, 211, 47-69, 2004.

473 Ji, W. B., Lin, W., Faure, M., Chen, Y., Chu, Y., Xu, Z. H.: Origin of the Late Jurassic to Early  
 474 Cretaceous peraluminous granitoids in the northeastern Hunan province (middle Yangtze  
 475 region), South China: Geodynamic implications for the Paleo-Pacific subduction, *J. Asian Earth*  
 476 *Sci.*, 141, 174-193, 2017.

477 Jiang, S. H., Bagas, L., and Liang, Q. L.: New insights into the petrogenesis of volcanic rocks in the  
 478 Shanghang Basin in the Fujian Province, China, *J. Asian Earth Sci.*, 105, 48-67, 2015.

479 Jiang, S. H., Liang, Q. L., Bagas, L., Wang, S. H., Nie, F. J., and Liu, Y. F.: Geodynamic setting of  
 480 the Zijinshan porphyry-epithermal Cu-Au-Mo-Ag ore system, SW Fujian Province, China:  
 481 constraints from the geochronology and geochemistry of the igneous rocks, *Ore Geol. Rev.*, 53,  
 482 287-305, 2013.

483 Jiang, W. S., Zhen, J. S., Li, L. T., and Xu, K. D.: Study of the Cretaceous in Zhejiang, China,  
 484 Nanjing, Nanjing University Press, 1-42 (in Chinese with English summary), 1993.

485 Jiang, Y. H., Wang, G. C., Liu, Z., Ni, C. Y., Qing, L., and Zhang, Q.: Repeated slab advance-retreat  
 486 of the Palaeo-Pacific plate underneath SE China, *Intl. Geol. Re.*, 57, 472-491, 2015.

487 Jiang, Y. H., Zhao, P., Zhou, Q., Liao, S. Y., and Jin, G. D.: Petrogenesis and tectonic implications  
 488 of Early Cretaceous S- and A-type granites in the northwest of the Gan-Hang rift, SE China,  
 489 *Lithos*, 121, 55-73, 2011.

490 Jiang, Y.H., Jiang, S.Y., Dai, B.Z., Liao, S.Y., Zhao, K.D., and Ling, H.F., 2009, Middle to Late  
 491 Jurassic felsic and mafic magmatism in southern Hunan Province, Southeast China:  
 492 implications for a continental arc to rifting: *Lithos*, vol. 107, p. 185-204.

493 Klötzli U, Klötzli E, Günes Z, and Kosler, J.: Accuracy of laser ablation U-Pb zircon dating: Results  
 494 from a test using five different reference zircons. *Geostand Geoanal Res*, 33, 5-15, 2009.

495 Lapierre, H., Jahn, B.M., Charvet, J., and Yu, Y. W.: Mesozoic felsic arc magmatism and continental  
 496 olivine tholeiites in Zhejiang Province and their relationship with tectonic activity in SE China,  
 497 *Tectonophysics*, 274, 321-338, 1997.

498 Lepvrier, C., Maluski, H., Maluski, H., Van Tich, V., Leyreloup, A., Thi, P. T., and Van Vuong, N.:  
 499 The Early Triassic Indosinian orogeny in Vietnam (Truong Son Belt and Kontum Massif);  
 500 implications for the geodynamic evolution of Indochina, *Tectonophysics*, 393(1-4), 87-118,  
 501 2004.

Li, C. L., Wang, Z. X., Wang, D. X., Cao, W. T., Yu, X. Q., Zhou, G. Z., and Gao, W. L.: Crust-mantle interaction triggered by oblique subduction of the Pacific plate: geochronological, geochemical, and Hf isotopic evidence from the Early Cretaceous volcanic rocks of Zhejiang Province, southeast China, *Intl. Geol. Rev.*, 56(14), 1732-1753, doi: 10.1080/00206814.2014.956347, 2014.

Li, J. H., Ma, Z. L., Zhang, Y. Q., Dong, S. W., Li, Y., Lu, M.A., and Tan, J. Q.: Tectonic evolution of Cretaceous extensional basins in Zhejiang Province, eastern South China: Structural and geochronological constraints, *Intl. Geol. Rev.*, 56(13), 1602-1629, doi: 10.1080/00206814.2014.951978, 2014.

Li, K. Y., Shen, J. L., and Wang, X. P.: Isotopic geochronology of Mesozoic terrestrial volcanic rocks in Zhejiang, Fujian and Jiangxi China, *J. Stratigr.*, 13(1), 1-13 (in Chinese with English abstract), 1989.

Li, S. Z., Suo, Y. H., Li, X. Y., Zhou, J., Santosh, M., Wang, P. C., Wang, G. Z., Guo, L. L., Yu, S. Y., Lan, H. Y., Dai, L. M., Zhou, Z. Z., Cao, X. Z., Zhu, J. J., Liu, B., Jiang, S. H., Wang, G., and Zhang, G. W.: Mesozoic tectono-magmatic response in the East Asian ocean-continent connection zone to subduction of the Paleo-Pacific Plate, *Earth-Sci. Rev.*, 192, 91-137, 2019.

Li, X. H. Cretaceous magmatism and lithospheric extension in Southeast China. *J. Asian Earth Sci.*, 18, 293-305, 2000.

Li, X. H., Liu, X. M., Liu, Y. S., Su, L., Sun, W. D., Huang, H. Q., and Yi, K.: Accuracy of LA-ICPMS zircon U-Pb age determination: An inter-laboratory comparison, *Sci. China Earth Sci.*, 58, 1722–1730, doi: 10.1007/s11430-015-5110-x, 2015.

Li, X. H., Zhang, C. K., Li, Y. X., Wang, Y., and Liu, L.: Refined chronostratigraphy of the late Mesozoic terrestrial strata in South China and its tectono-stratigraphic evolution, *Gond. Res.*, 66, 143-167, 2019.

Li, Z. X., and Li, X. H.: Formation of the 1300-km-wide intercontinental orogen and postorogenic magmatic province in Mesozoic South China: A flat-slab subduction model, *Geology*, 35, 179-182, 2007.

Liu, K., Zhang, J. J., Wilde, S. A., Zhou, J. B., Wang, M., Ge, M. H., Wang, J. M., and Ling, Y. Y.: Initial subduction of the Paleo-Pacific Oceanic plate in NE China: Constraints from whole-rock geochemistry and zircon U-Pb and Lu-Hf isotopes of the Khanka Lake granitoids, *Lithos*, 274-275, 254-270, 2017.

Liu, L., Xu, X. S., and Xia, Y.: Asynchronizing paleo-Pacific slab rollback beneath SE China: Insights from the episodic Late Mesozoic volcanism, *Gond. Res.*, 37, 397-407, 2016.

Liu, L., Xu, X. S., and Xia, Y.: Cretaceous Pacific plate movement beneath SE China: Evidence from

536 episodic volcanism and related intrusions, *Tectonophysics*, 614, 170-184, 2014.

537 Liu, L., Xu, X. S., and Zou, H. B. Episodic eruptions of the Late Mesozoic volcanic sequences in  
538 southeastern Zhejiang, SE China: petrogenesis and implications for the geodynamics of  
539 paleo-Pacific subduction, *Lithos*, 154, 166-180, 2012.

540 Ludwig, K. R.: *Squid 1.02: A User's Manual* (2), Berkeley Geochron. Centre, Special Publication,  
541 1-19, 2001.

542 Ma, Z. L., Li, J. H., Zhang, Y. Q., Dong, S. W., Song, C. Z., and Li, Y.: Geochronological and  
543 structural constraints on the lithostratigraphic units of the Lishui Basin, southeastern China,  
544 *Geol. China*, 43(1), 56-71 (in Chinese with English abstract), 2016.

545 Meng, L. F., Li, Z. X., Chen, H. L., Li, X. H., and Wang, X. C.: Geochronological and geochemical  
546 results from Mesozoic basalts in southern South China Block support the flat-slab subduction  
547 model, *Lithos*, 132-133, 127-140, 2012.

548 Qiu, Y. M., Gao, S., McNaughton, N. J., Groves, D. I., and Ling, W. L.: First evidence of N3.2 Ga  
549 continental crust in the Yangtze Craton of South China and its implications for Archean crustal  
550 evolution and Phanerozoic tectonics, *Geology*, 28(1), 11-14, 2000.

551 Schoene, B., Condon, D. J., Morgan, L., and McLean, N.: Precision and Accuracy in Geochronology,  
552 *Elements*, 9, 19-24, doi: 10.2113/gselements.9.1.19, 2013.

553 Sha, J. G. *Plicatounio* from Hekou Formation of Hekou basin, Ninghua, Fujian, with discussion on  
554 classification of Plicatounionidae, *Acta Palaeont. Sin.*, 29(4), 472-489 (in Chinese with English  
555 abstract), 1990.

556 Shu, L. S., Zhou, X. M., Deng, P., Wang, B., Jiang, S. Y., Yu, J. H., and Zhao, X. X.: Mesozoic  
557 tectonic evolution of the Southeast China Block, New insights from basin analysis, *J. Asian*  
558 *Earth Sci.*, 34, 376-391, 2009.

559 Shu, X., Yang, S. Y., Jiang, S. Y., and Ye, M. Petrogenesis and geodynamic setting of Early  
560 Cretaceous felsic rocks in the Gan-Hang Belt, Southeast China: Constraints from  
561 geochronology and geochemistry of the tuffs and trachyandesitic rocks in Shengyuan volcanic  
562 Basin, *Lithos*, 284-285, 691-708, 2017.

563 Solari, L. A., Gómez-Tuena, A., Bernal, J. P., Pérez-Arvizu, O., and Tanner, M.: U-Pb zircon  
564 geochronology with an integrated LA-ICP-MS microanalytical workstation: Achievements in  
565 precision and accuracy, *Geostand Geoanal Res*, 34, 5-18, 2010.

566 Stepashko, A. A.: The Cretaceous Dynamics of the Pacific Plate and Stages of Magmatic Activity in  
567 Northeastern Asia, *Geotectonics*, 40(3), 225-235, 2006.

568 Sun, M. D., Chen, H. L., Zhang, F. Q., Wilde, S. A., Dong, C. W., and Yang, S. F.: A 100 Ma  
569 bimodal composite dyke complex in the Jiamusi Block, NE China: An indication for

lithospheric extension driven by Paleo-Pacific roll-back, *Lithos*, 162, 317-330, 2013.

Sun, M. D., Xu, Y. G., Wilde, S. A., and Chen H. L.: Provenance of Cretaceous trench slope sediments from the Mesozoic Wandashan Orogen, NE China: Implications for determining ancient drainage systems and tectonics of the Paleo-Pacific, *Tectonics*, 34, 1269-1289, doi:10.1002/2015TC003870, 2015.

Sun, W. D., Ding, X., Hu, Y. H., and Li, X. H.: The golden transformation of the Cretaceous plate subduction in the west Pacific, *Earth-Planet. Sci. Lett.*, 262, 533-542, 2007.

Taylor, B., and Hayes, D.E.: Origin and history of the South China Sea Basin: *in* Hayes, D. E., Ed., *The Tectonic and Geologic Evolution of Southeast Asian Seas and Islands: Part 2*, Am. Geophys. Union Geophys. Monograph, 27, 23-56, 1983.

Wang, D. Z., Zhou, J. C., Qiu, J. S., and Fan, H. H.: Characteristics and petrogenesis of late Mesozoic granitic volcanic-intrusive complexes in southeastern China, *Geol. J. China Uni.*, 6(4), 487-798 (in Chinese with English abstract), 2000.

Wang, G. C., Jiang, Y. H., Liu, Z., Ni, C. Y., Qing, L., Zhang, Q., and Zhu, S. Q.: Multiple origins for the Middle Jurassic to Early Cretaceous high-K calc-alkaline I-type granites in northwestern Fujian province, SE China and tectonic implications, *Lithos*, 246-247, 197-211, 2016.

Wang, X. L., Zhou, J. C., Qiu, J. S., Zhang, W. L., Liu, X. M., and Zhang, G. L.: LA-ICPMS U–Pb zircon geochronology of the Neoproterozoic igneous rocks from Northern Guangxi, South China: implications for tectonic evolution, *Precambrian Res.*, 145 (1-2), 111-130, 2006.

Wang, Y. J., Fan, W. M., Cawood, P. A., Li, S. Z.: Sr–Nd–Pb isotope constraints on multiple mantle domains for Mesozoic mafic rocks beneath the South China Block hinterland, *Lithos* 106, 297-308, 2008.

Wang, Y. J., Fan, W. M., Zhang, G. W., and Zhang, Y. H.: Phanerozoic tectonics of the South China Block: Key observations and controversies, *Gond. Res.*, 23, 1273-1305, doi: 10.1016/j.gr.2012.02.019, 2013.

Wu, F., Yang, J., Lo, C., Wilde, S. A., Sun, D., and Jahn, B.: The Heilongjiang Group: a Jurassic accretionary complex in the Jiamusi Massif at the western Pacific margin of northeastern China, *Island Arc*, 16, 156-172, 2007.

Wu, J. H., Liu, F. Y., and Liu, Sh.: SHRIMP U-Pb Zircon Age of Late Mesozoic Trachyte in Xiajiang—Guangfeng and Sannan (Quannan, Dingnan and Longnan)—Xunwu Volcanic Belts, *Geol. Rev.*, 57(1), 125-132 (in Chinese with English abstract), 2011a.

Wu, J. H., Xiang, Y. X., and Liu, S.: Wuyi Group of southern Jiangxi and its geological age, *J. Stratigr.*, 35(2), 200-208 (in Chinese with English abstract), 2011b.

Wu, J., and Wu, J. H.: Shuangfengling formation in Jiangxi and its geological age, *J. East China Inst.*

Techn., 36, 17-24 (in Chinese with English abstract), 2013.

Xie, J. C., Fang, D., Xia, D., Li, Q. Z., and Sun, W. D.: Petrogenesis and tectonic implications of late Mesozoic granitoids in southern Anhui Province, southeastern China, *Intl. Geol. Rev.*, 59(14), 1804-1826, doi: 10.1080/00206814.2017.1297964, 2017.

Yang, J. B., Zhao, Z. D., Hou, Q. Y., Niu, Y. L., Mo, X. X., Sheng, D., and Wang, L. L.: Petrogenesis of Cretaceous (133–84 Ma) intermediate dykes and host granites in southeastern China: Implications for lithospheric extension, continental crustal growth, and geodynamics of Palaeo-Pacific subduction, *Lithos*, 296-299, 195–211, 2018.

Yang, S. Y., Jiang, S. Y., Zhao, K. D., Jiang, Y. H., Ling, H. F., and Luo, L.: Geochronology, geochemistry and tectonic significance of two Early Cretaceous A-type granites in the Gan-Hang Belt, Southeast China, *Lithos*, 150, 155-170, 2012.

Yang, Y. L., Ni, P., Yan, J., Wu, C. Z., Dai, B. Z., and Yu, Y. F.: Early to late Yanshanian I-type granites in Fujian Province, SE China: Implications for the tectonic setting and Mo mineralization, *J. Asian Earth Sci.*, 137, 194-219, 2017.

Yu, X. Q., Shu, L. S., Deng, P., Wang, B., and Zhu, F. P.: The sedimentary features of the Jurassic-Tertiary terrestrial strata in southeast China, *J. Stratigr.*, 27(3), 254-263 (in Chinese with English abstract), 2003.

Zhang, B., Guo, F., Zhang, X. B., Wu, Y. M., Wang, G. Q., and Zhao, L.: Early Cretaceous subduction of Paleo-Pacific Ocean in the coastal region of SE China: Petrological and geochemical constraints from the mafic intrusions, *Lithos*, 334-335, 8-24, 2019.

Zhang, C., Ma, C. Q., Liao, Q. N., Zhang, J. Y., and She, Z. B.: Implications of subduction and subduction zone migration of the Paleo-Pacific Plate beneath eastern North China, based on distribution, geochronology, and geochemistry of Late Mesozoic volcanic rocks, *Intl. J. Earth Sci. (Geol Rundsch)*, 100, 1665-1684, 2011.

Zhang, J. H., Yang, J. H., Chen, J. Y., Wu, F. Y., and Wilde, S. A.: Genesis of late Early Cretaceous high-silica rhyolites in eastern Zhejiang Province, southeast China: A crystal mush origin with mantle input, *Lithos*, 296-299, 482-495, 2018.

Zhang, L. M.: The Jurassic-Cretaceous boundary in the Zhejiang-Fujian-Jiangxi region, *Geol. Rev.*, 43(1), 25-31 (in Chinese with English abstract), 1997.

Zhao, G. C., and Cawood, P. A.: Tectonothermal evolution of the Mayuan assemblage in the Cathaysia Block: new evidence for Neoproterozoic collisional-related assembly of the South China craton, *Am. J. Sci.*, 299, 309-339, 1999.

Zhao, J. L., Qiu, J. S., Liu, L., and Wang, R. Q.: The Late Cretaceous I- and A-type granite association of southeast China: Implications for the origin and evolution of post-collisional



638 extensional magmatism, *Lithos*, 240-243, 16-33, doi: [org/10.1016/j.lithos.2015.10.018](https://doi.org/10.1016/j.lithos.2015.10.018), 2016.

639 Zheng, Y. F., and Zhang, S. B.: Formation and evolution of Precambrian continental crust in South  
640 China, *Chinese Sci. Bull.*, 52, 1-12, 2007.

641 Zhou, X. M., and Li, W. X.: Origin of Late Mesozoic igneous rocks in southeastern China:  
642 implications for lithosphere subduction and underplating of mafic magmas, *Tectonophysics*, 326,  
643 269-287, 2000.

644 Zhou, X. M., Sun, T., Shen, W. Z., Shu, L. S., Niu, Y. L.: Petrogenesis of Mesozoic granitoids and  
645 volcanic rocks in South China: a response to tectonic evolution, *Episodes*, 29(1), 26-33, 2006.

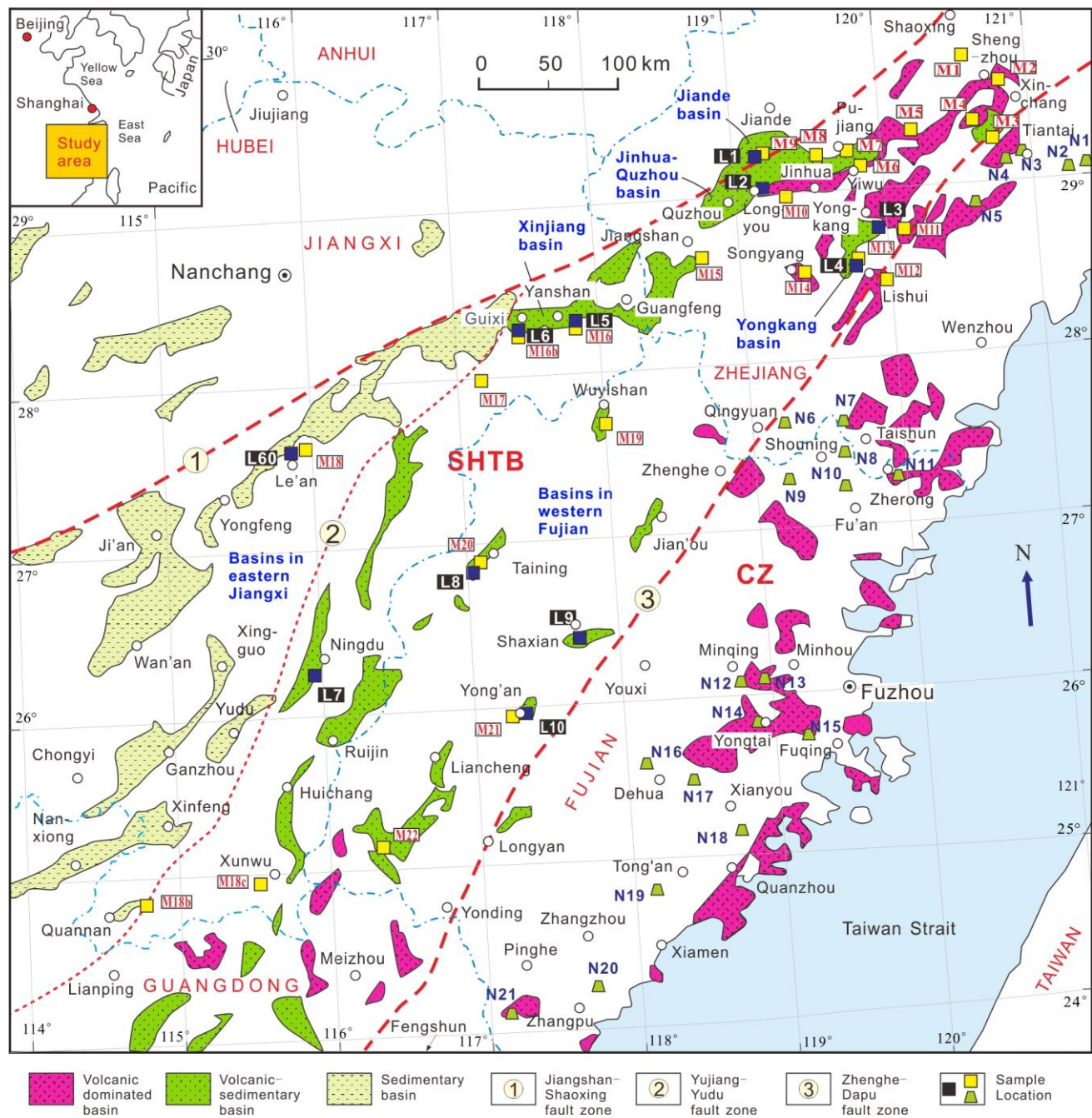
646

647 **Tables**

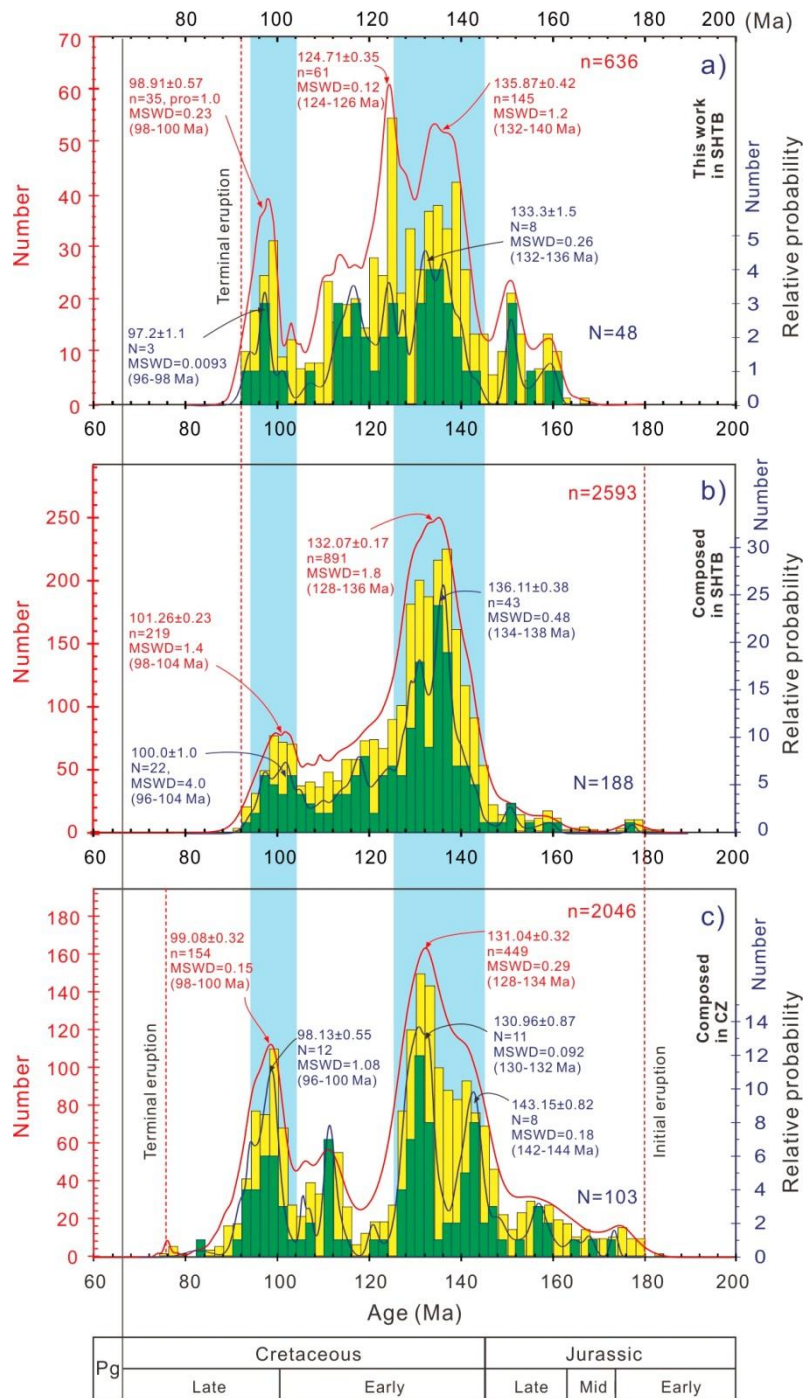
648 Table 1 Percentages of single zircons and rock samples in 1σ error (Myr), error/age ratio, and Th/U  
649 ratio of the late Mesozoic extrusive rocks in SE China

Sources	Con- cordant zircon Number	Rock Sample	1σ error						error/age						Zircon Number (Th/U)	Th/U		
			Age (Myr)	Zircon Number	%	Age (Myr)	Sample Numbe r	%	Rati o	Zircon Number	%	Age (Myr)	Sample Number	%		Ratio	Zircon Number	%
This work in SHTZ	636	48	<3	570	89.6	<2	46	95.8	0-3	581	91.4	<2	41	85.4	636	<0.1	1	0.2
			3-5	63	9.9	2-4	2	4.2	3-5	50	7.9	2-4	7	14.6		0.1-1.0	20	3.1
			>5	3	0.5	>4			>5	5	0.8	>4				1.0-10	615	96.7
																>10	0	0.0
Composed in SHTZ	2593	188	<3	2066	79.7	<2	153	81.4	0-3	2212	85.3	<2	168	89.4	2503	<0.1	1	0.0
			3-5	441	17.0	2-4	31	16.5	3-5	348	13.4	2-4	18	9.6		0.1-1.0	945	37.8
			>5	86	3.3	>4	4	2.1	>5	33	1.3	>4	2	1.1		1.0-10	1543	61.6
																>10	14	0.6
Composed in SHTZ+C Z	4639	291	<3	3543	76.4	<2	246	84.5	0-3	3798	81.9	<2	264	90.7	4175	<0.1	1	0.0
			3-5	898	19.4	2-4	39	13.4	3-5	769	16.6	2-4	25	8.6		0.1-1.0	1766	42.3
			>5	198	4.3	>4	6	2.1	>5	73	1.6	>4	2	0.7		1.0-10	2394	57.3
																>10	14	0.3

Notes: Numbers of evaluated zircon grains differ from sources in U-Pb age and Th/U ratio due to unavailability of some original dada. CZ, Coastal zone;



656 Figure 1 Sketch geological map of South China showing tectonic and basin zonation of the upper  
657 Mesozoic and sample locations (map simplified after Shu et al., 2009). In SHTB (Shi-Hang tectonic  
658 belt), dark blue squares with white capital letter L + numbers within black rectangles mark the  
659 sampling locations of this study (supplementary data figures RD1, RD2, and RD3), and yellow  
660 squares with red capital letter M + numbers within white rectangles indicate sampling locations of  
661 previous studies (supplementary data Table RD1 and RD2). In CZ (Coastal Zone), green trapezoids  
662 with bold capital letter N + numbers are sample locations of previous studies (supplementary data  
663 Table RD1 and RD3).



664

665 Figure 2 Relative probability and histogram diagrams of concordant zircon U-Pb isotope and  
 666 sample weighed-mean ages of extrusive rocks from SE China (details see in supplementary data  
 667 Table RD1, RD2, and RD3). a), this study in the SHTB; b), combined this and previous studies in the  
 668 SHTB; c), published data in the CZ. N = number of rock samples, n = total number of zircon grains.

669

670

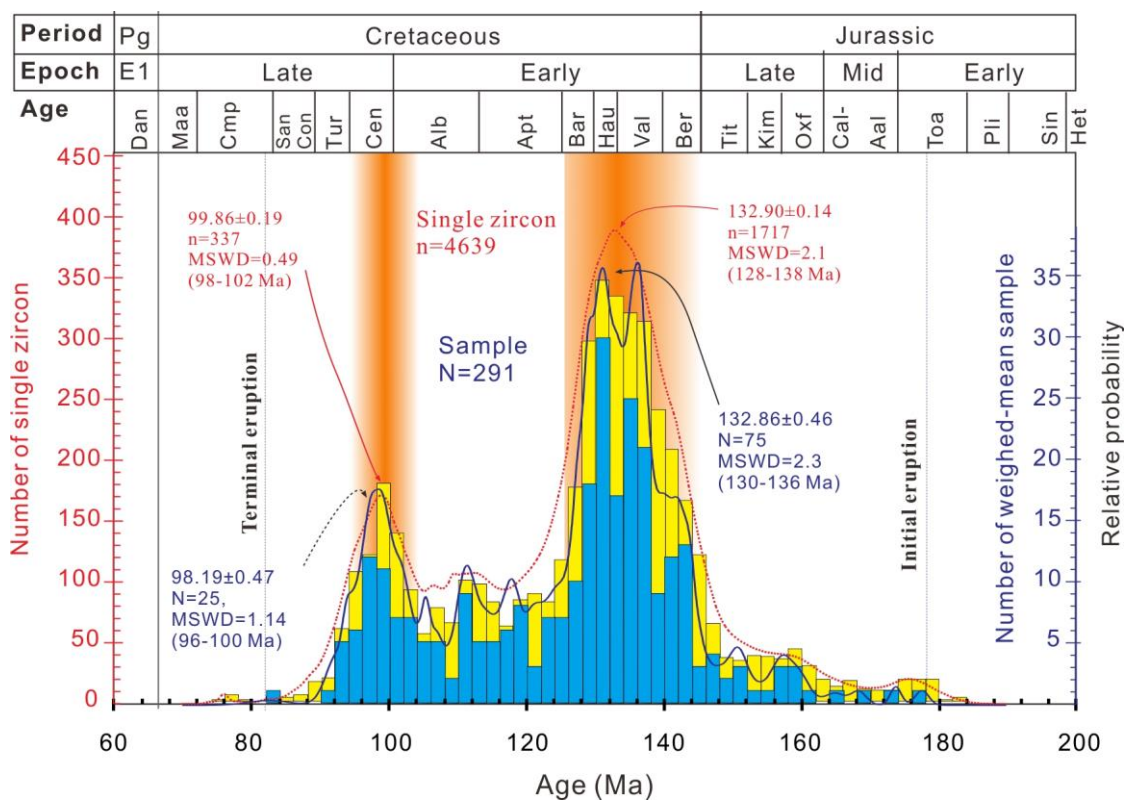
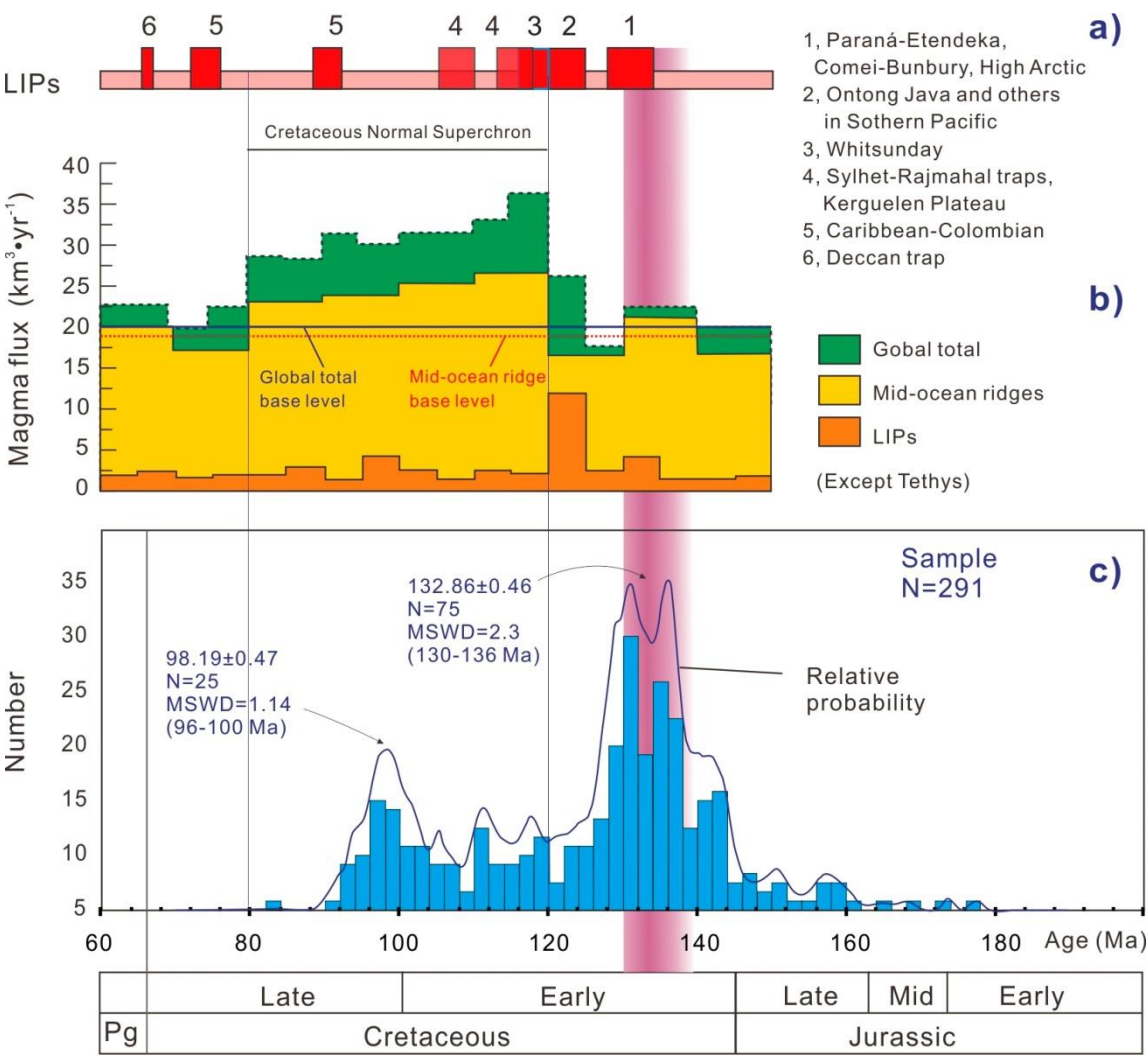


Figure 3 Diagram showing U-Pb isotope age relative probability and histogram of both single zircon and individual sample weighed mean zircons from all extrusive rock samples in SE China. N = number of rock samples, n = total number of zircon grains.





685 Figure 4 Diagram showing age ranges of volcanism in SE China and correlations with the global  
686 Large Igneous Provinces (LIPs) and magmatic flux. a, age range of the Cretaceous LIPs (summary  
687 see Coffin & Eldholm, 1994); b, magma flux of the Cretaceous LIPs, mid-ocean ridges, and (except  
688 Tethys) global total (Coffin & Eldholm, 1994); c, age range of the volcanism with histogram and  
689 relative probability and SE China.

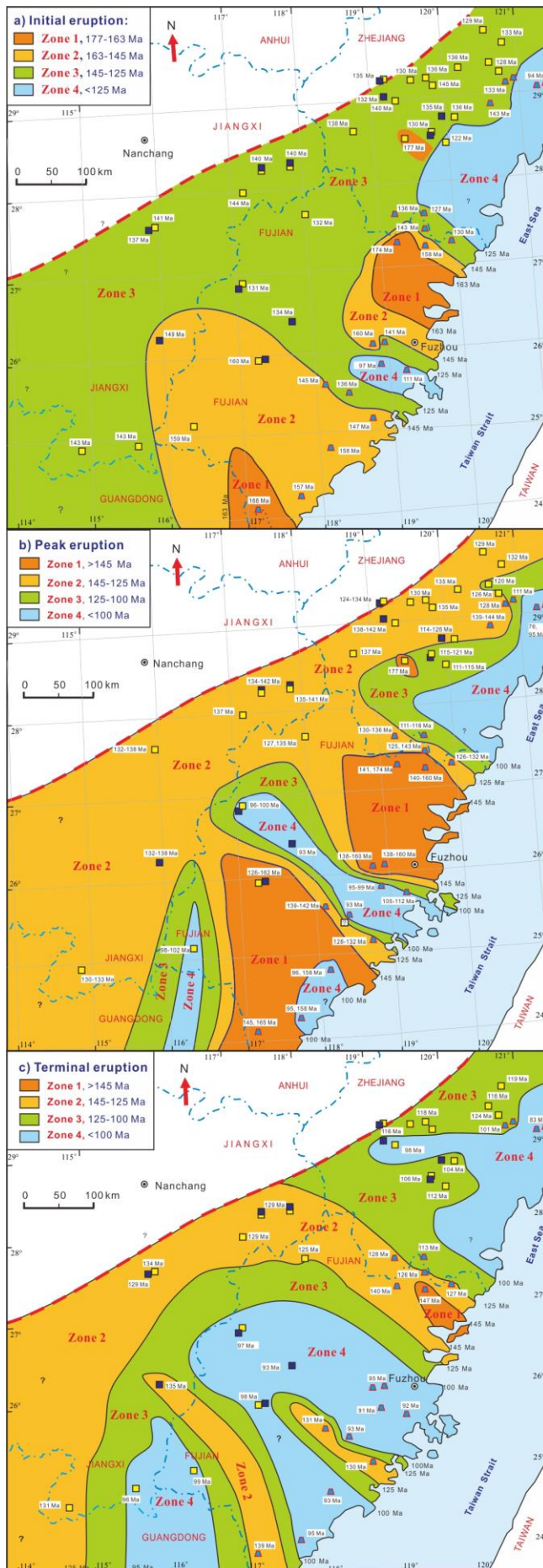


Figure 5 Sketch maps showing zonations of the late Mesozoic volcanism by age in SE China. Age within white rectangles is the eruption time at a location or in a basin/region. Names of color squares and trapezoids refer to Fig. 1. a), zonations of initial eruption ages; b) zonations of peak eruption ages; c) zonations of terminal eruption ages.